Relativistic Density Functional Study on Uranium(IV) and Thorium(IV) Oxide Clusters of Zonohedral Geometry

Grigory A. Shamov*,[†,‡]

[†]Department of Chemistry, University of Manitoba, Winnipeg MB, Canada R3T 2N2

[‡]Division of Informational Technologies, Kazan National Research Technological University, Kazan, Karl Marx str. 18, 420015 Russian Federation

S *Supporting Information*

ABSTRACT: Free and ligated oxide clusters of thorium(IV) and uranium(IV) were studied with density functional theory using all-electron scalar relativistic method, as well as energy-consistent relativistic *f*-in-core pseudopotentials. The main driving force for the cluster formation is the sintering of the dioxoactinide moieties, which is more favorable for thorium(IV) than for uranium(IV) because, for the latter, a penalty for bending of the uranyl(IV) is to be paid. We assumed that the rhombic structural motif that exists already in the $(AnO_2)_2$ dimer could be a guide to explaining the preference for the existing An_6O_8-type clusters. On the basis of this, we have theoretically explored the possibility of the existence of similar (zonohedric) polyhedral actinide oxide clusters and found that the next possible cluster would be of $An_{12}O_{20}$ stoicheometry. We have predicted by our DFT computations that the corresponding zonohedral clusters would be minima on the potential energy surface. The alternating An−O rhombic structural motif also offers a possible explanation of the existence and stoichiometry of the only nonfluorite cluster thus far, the $An_{12}O_{20}$, which is nonzonohedral, nonconvex, but still a rhombic polyhedron. Our relativistic all electron DFT computations of both free cationic and ligated clusters predict that preparation of the larger clusters is not forbidden thermodynamically. We have also found that for the uranium(IV), oxide dimer and hexamer clusters are antiferromagnetic, broken spin singlet in their ground state, while ligated $[U_6O_8]$ clusters prefer an all high-spin electronic configuration.
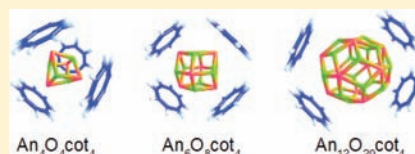
INTRODUCTION

In the past decade, there has been a renaissance of actinide chemistry, both experimental and theoretical, with the opening of several completely new research venues. One of the most exciting developments on the frontier has been the emergence of actinide-based nanostructured materials, such as nanotubes of actinyl borates and selenates, nanoclusters of actinyl peroxides, and inorganic framework materials based on them.[1] The new materials hold great practical promise as framework materials with the internal surface properties competitive with zeolites and MOFs.[2−4] Among the other nanostructures that have been discovered in the past few years were well-defined oxide and peroxide clusters of early actinides in oxidation degrees IV, V, and VI correspondingly. In this study, we will try to model computationally the structure and thermodynamics of the small oxide clusters of uranium(IV) and their thorium(IV) analogs.

Recently, Burns and co-workers[5,6] discovered the method of preparation of more than 50 distinct, well-defined spherical uranyl(VI) peroxide clusters, ranging from 20 to 60 uranyl units. The peroxide clusters are built from fused four- to six-membered rings, with edges made of the side-on bridging peroxide dianions, hydroxides, and in some cases, additional ligands like oxalates of phosphates. These clusters have the potential to be used in new actinide separation and spent nuclear fuel reprocessing applications. Factors determining the stability of the actinyl peroxide clusters are still not completely understood. Favoring of high symmetry structures and preference for clusters built of five-membered rings were proposed as the factors in earlier works by Burns et al., but since then, they synthesized clusters with supposedly strained four-membered rings, as well as structures of lower symmetries. The direct *ab initio* theoretical modeling of these clusters is yet out of reach due to their large size and the necessity to include solvent and counterions into the model system. A set of smaller models consisting of the building block units of uranyl peroxide clusters have been recently studied theoretically in two parallel works published in 2010, by Gagliardi et al. and Bo et al.[7,8] It was shown that cluster formation is facilitated by the inherently bent character of the side-on peroxide bridge (although a preference over the planar one is just 0.5 kcal/mol) and by the templating influence of counterions.

Oxide clusters of the four-valent actinides are still less studied than uranyl peroxide clusters; however, the knowledge here is quickly expanding. The practical importance of these systems is high: the low-valent clusters of actinides that have unpaired f electrons are of importance as molecular magnets;[9] they are also of relevance in the development of new nuclear materials and also as models of environmentally relevant low-valent actinide species and colloids.[10,11]

To date, several stable oxide clusters of tetravalent actinides have been reported. They do not show the structural diversity of the peroxide clusters of actinyls(VI). The most frequently

occurring clusters are of the $[An_6O_8]X_n$ type. The cluster's core is of rhombohedric geometry (Figure 1a) and represents a
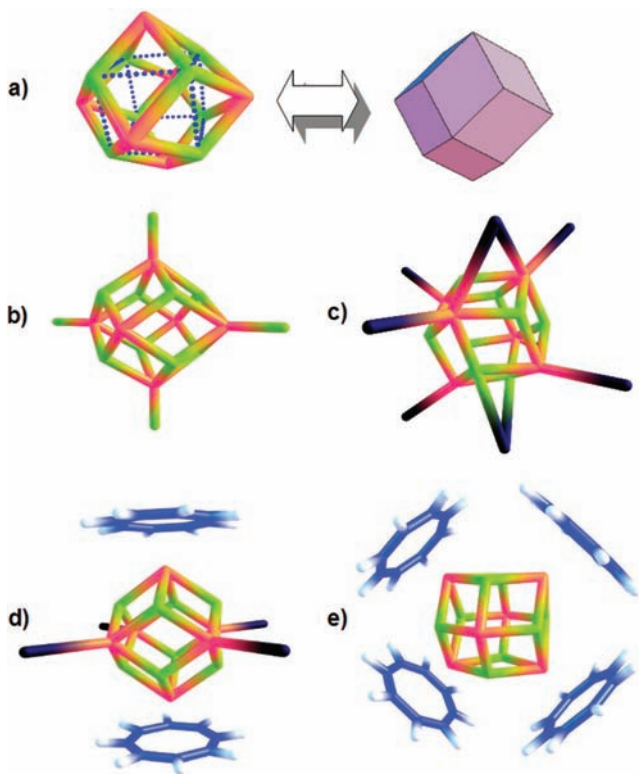
Figure 1. (a) The free fluorite-structure $An_6O_8{}^{8+}$ cluster, a rhombohedron. PBE/L1 optimized geometries of its ligated forms considered in this paper for An═Th are shown for (b) the tetraoxo-compound $(ThO_2)_6$, (c) $An_6O_8I_8$, (d) $An_6O_8I_4(COT)_2$, and (e) $An_6O_8(COT)_4$. Oxygen atoms are in green-yellow, thoriums in pink, carbon in blue, hydrogen in light-blue, and iodine in dark-violet.

fragment of the solid AnO_2 oxide with a fluorite structure: an octahedron of actinide atoms included in a cube of oxygen atoms.[12] For the uranium(IV), it was first prepared by conproportionation of uranium(III) salts with uranyl(VI) and in the presence of polydentate ligands by Berthet et al.[13] Recently, it was found by the same group that the U_6O_8-type clusters with various chelates, as well as monodentate or other nonbridging ligands such as iodide ions or cyclooctatetranyl (COT) dianions, can be easily prepared by the reaction of uranocene with uranyl salts in nonaqueous media (pyridine); in this case, the cyclooctatetraenyl ligand acts as the reductant of the uranyls as in eq 1.[14] Moreover, they have shown that ligand exchange reactions, such as furnishing an iodide-ligated $[U_6O_8]$ cluster with a COT ligand, can be performed.

$$4U^{(VI)}O_2X_2 + 2COT_2U^{(IV)} \rightarrow U^{(IV)}{}_6O_8X_8 + 4COT \qquad (1)$$
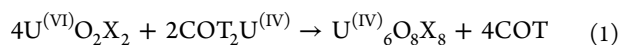
To date, several research groups have prepared similar hexanuclear uranium clusters. Mazzanti and co-workers did it by controlled hydrolysis of uranium(III) salts in nonaqueous media.[15] Also, larger clusters of the fluorite structure, i.e., built of two or three fused U_6O_8 units, U_{10} and U_{16}, correspondingly, and a different cluster with nonfluorite, the $[U_{12}O_{20}]$ core, were obtained[16,17,16] using this method. Bridged ligands such as triflates always cover the clusters. The cleavage of the larger clusters induced by the change of chelating ligands and leading to the smaller $[U_6O_8]$ ones has been observed.[17] Interestingly,

the clusters obtained by this method are reported to be partially protonated and to be therefore mixed-valence U(IV)/U(V) compounds. The $[U_{12}O_{20}]$ cluster that is, to our knowledge, the only nonfluorite uranium(IV) oxide cluster known has eight protons attached to the bridging oxygens in a symmetric fashion.

The actinide(IV) clusters belong not only to strictly nonaqueous chemistry. The clusters of both $U_6O_8{}^{8+}$ and $Th_6O_8{}^{8+}$, with the bridging formate ligands, were obtained by a pH change from corresponding aqueous An(IV) compounds in aqueous media.[18] For plutonium, the oxidation state of four is the predominant one; Soderholm et al. found that plutonium-(IV) oxide in aqueous solution exists in the form of larger fluorite clusters.[19,20] A well-defined plutonium oxide cluster of the fluorite structure covered with monodentate chloride ligands, $Pu_{38}O_{56}Cl_{54}$, has been characterized by them in ref 20. Very recently, $[Th_6O_8]$ clusters in their protonated forms were obtained, also by hydrolysis, and studied computationally in ref 21; the computation study was done using effective core potentials (ECP) and was dedicated to the location of the protonation sites in the cluster.

Despite the significant progress in experimental studies of the oxide actinyl(IV) clusters, the available experimental data are still controversial. The role of the bridging first-coordination sphere ligands is not clear. It was originally assumed that they are required for the stabilization of the $[U_6O_8]$ core because most of the clusters had either triflate of formiate ligands.[13,15,18] However, the synthesis from uranocene, by Berthet et al., that leads to stable clusters with nonbridging ligands such as iodide, cyclooctatetraene, THF, and pyridine, seems to suggest otherwise.[14] At the same time, it was found that the larger deca- and hexadeca-nuclear uranium(IV) clusters can be cleaved with the ligand changes, forming the smaller U_6O_8 clusters, which then decompose.[17] A controversy exists for the composition and oxidation degree of uranium U_6O_8 clusters, which perhaps depends on the synthetic pathway from they were obtained. Mazzanti et al. report the clusters as being a mixed-valence species with some U(V) content.[16,17,15] On the other hand, the pH-controlled experiments yielded similar clusters for both uranium and thorium, while the latter, obviously, cannot be of valence higher than four.[18,21] Extracting the oxidation state of the uranium directly from the magnetic measures of the U(IV) clusters' magnetism is difficult due to the complex interplay of the spin−orbit and exchange interactions. Finally, it is not yet clear if all actinide(IV) oxides are to be of the fluorite structure following the structural patterns of the solid metal dioxides, or whether a richer structural chemistry can be realized as in the case of actinyl(VI) peroxides. Therefore, a theoretical modeling of the thermody-namics of these clusters and their geometric and electronic structure might be useful for achieving an understanding of the available experimental data, for the prediction and rational design of the actinide nanomaterials.

The theoretical modeling of actinide(IV) clusters, to our knowledge, has been so far quite scarce and dedicated to thorium systems. An extended Hueckel method computation was done on a thorium nitride cluster.[22] Very recently, Schimmelpfennig reported a computation using very large core pseudopotentials of a nanometer-scale thorium oxide cluster of 146 actinide atoms with DFT.[23] The most recent computational studies that were done by Dixon et al. apply small-core pseudopotentials for the $[Th_6O_8]$ clusters[21] and also

for the small Th_2O_4 cluster,[24] which was experimentally studied by IR spectroscopy in a noble-gas matrix.

In the present work, we will study the electronic structure and thermodynamics of the free and ligated $An_6O_8^{8+}$ (An = Th, U) clusters using relativistic all-electron density functional methods. Effects of the environment can be very strong and probably dominate the formation of complexes and clusters of actinyls(V) and (VI) (cf. our works on actinyl hydration energies[25,26] and crowns[27]). However, since the oxide actinide-(IV) clusters can be prepared in both aqueous and nonaqueous solvents, it would be meaningful to study them first by themselves in their isolated gas-phase form. We will also probe whether there are possible different nonfluorite structures that are larger and smaller than the $[U_6O_8]$ cluster core. In order to simplify the computation procedure, we will start from the clusters of the f^0-Th(IV), then computing corresponding U(IV) systems whenever feasible.

■ COMPUTATIONAL DETAILS

Modeling of the actinide oxide clusters meets the usual challenges of theoretical actinide chemistry: the need for the treatment of relativistic effects and the large size of the model systems that contain a large number of electrons. For the open-shell, early actinide systems such as UO_2 and, by extension, the uranyl(IV) oxide clusters, which have unpaired f electrons, as well as closely lying manifolds of f, d, and s levels, an accurate description of the energy levels is even more difficult due to the importance of both spin−orbit and multiplet/nondynamic correlation effects. In fact, the electronic structure of the uranium dioxide molecule was the subject of a controversy due to both experimental[28] and theoretical difficulties.[29−31] We note that the reliable relativistic Fock-space coupled-cluster method from ref 31 is too expensive to be routinely applied to larger actinide clusters we would like to study, and CASPT2 or its cheaper variants (ORMAS multireference MP2 techniques, for example) are not size-extensive methods and thus have limited use for thermodynamics of the actinide clusters. Thus, we chose density functional theory (DFT) as the only practical electronic structure method. With DFT being a single-determinant method, and with usual approximate density functionals like GGA, there is not much hope for it in complicated cases such as UO_2; instead, we were trying to get the lowest electronic state for the DFT method we used, as given by it. We have assumed that all thorium systems studied in this paper are closed-shell and treated them with the restricted SCF (RHF or RKS) method; for the uranium dioxide and uranium oxide clusters, we generally assumed that they must be in a high-spin state (two alpha electrons per uranium atom) and used the unrestricted SCF variant (UHF, UKS). In a few selected cases such as the UO_2 dimer, we have systematically explored spin-states other than the high-spin one.

In this work, we employ all-electron scalar relativistic, four component DFT methodology that we, and others, have previously used with success for modeling of the actinide compounds.[27,32−34] See the above references for a more detailed account. Unless otherwise noted, the all-electron four component scalar relativistic method as implemented in Priroda code version 6[35−39] was used. The relativistic method had been thoroughly benchmarked[25,40,41] earlier and was found to be reliable. All of the all-electron (AE) computations employed an ANO−DZP quality orbital basis set L1,[37] along with the corresponding small-component basis set obtained by the kinetic-balance condition and an optimized density fitting basis for resolution of the identity computation of the Coulomb and exchange DFT integrals, as supplied with the Priroda code. The size of the clusters precludes usage of the all-electron basis sets of higher quality rather than the ANO−DZP type bases L1 we used here.

Significant computational savings can be achieved by using the pseudopotential approach that removes core electrons from explicit computations. For actinides, several sets of pseudopotentials[42] in the form of the effective core potentials (ECP) exist. It was noted[43,25,27,40] that a "small-core" ECP is needed to describe processes that change the oxidation state of the actinides, such as their red-ox reactions in solution or the thermodynamics of homolytic dissociation of their oxides and fluorides. The available and widely used small-core, energy-consistent ECP (SC-ECP) set that spans the whole actinide series is the one from the Stuttgart−Dresden group.[44] However, a recent attempt had been made to prepare a "very large core" (VLC-ECP) with f-in-core to model systems within a given oxidation state.[45−47] Such pseudopotentials would offer much larger savings due to reducing the size of the model system, and would lift the typical convergence problems that plague the modeling of (especially polynuclear) complexes of the f elements. These pseudopotentials were applied to actinocenes, predicting the geometry successfully.[48]

In order to test the feasibility and accuracy of the ECP approach, we did computations using the VLC-ECP set for actinide atoms. Since the model system is smaller as a result of employing the pseudopotentials, we have used segmented triple-ζ polarized quality bases as follows. For the light elements, we used a segmented TZP basis, together with the corresponding density fitting basis set as provided in the Priroda code.[49] For the VLC-ECP, we took the An(IV) ECP by Moritz et al.[45] and corresponding TZP basis set from the Stuttgart pseudopotentials Web site.[50] An uncontracted nonoptimized fitting set of the (10s,10p, 10d, 9f, 7g) size was used. For the iodine atoms, we used the def-TZP set with corresponding JK-fitting basis set,[51] and the large-core pseudopotential from the Stuttgart group,[52] as taken from the TURBOMOLE basis library Web site.[53]

The PBE density functional[54] that shows good overall performance for the larger set of chemical problems[55] was used throughout this work. The only exception was in the case of AnO_2 and An_2O_4, for which we report also the results obtained with the hybrid PBE0 functional.[56]

Full, unconstrained geometry optimizations employing analytical gradients were performed without imposing symmetry constraints. Analytical second derivatives were computed to check the nature of the stationary points obtained from the optimizations, in most of the cases (unless explicitly noted in the text). The second derivatives were used to compute thermal components of the Gibbs free energy using a standard harmonic approximation; we chose the standard conditions of 298.15 K and 1 atm.

■ RESULTS AND DISCUSSION

Energetics and Electronic Structure of the $[An_6O_8]$ and $(AnO_2)_2$ Clusters. It is well-known that convergence of the SCF procedure for the polynuclear complexes and clusters of the f elements like U(IV) poses a serious problem. The problem is due to a manifold of closely lying f, d, and s shells that are available for occupation by the unpaired electrons, and often the multiconfigurational nature of these systems. Thus, we have first chosen to model the thorium(IV) clusters, which do not have f electrons, as a model of uranium clusters that are mostly studied experimentally. We note that Th_6O_8 clusters were also observed in the experiment along with U_6O_8 analogs.[18,21] We then tried to compute the corresponding uranium(IV) clusters, which we report for the cases where the SCF convergence was possible.

In the original experimental paper by Berthet et al., the oxidation of the cyclooctatetraenyl dianions ($COT^{2−}$) by uranyl(VI) was pointed to as the driving force of the process of the hexanuclear cluster formation according to eq 1. Such an oxidation is indeed an important factor. Our PBE/L1 computations estimate the energy of the corresponding process, reaction eq 2, to be −578.9 kcal/mol. Note that GGA DFT is likely to overestimate the energy of reduction of the dianions; on the other hand, the lack of spin−orbit interactions in our computation might underestimate the stability of the U(IV) dioxide to a few kcal/mol.[40]

$$COT^{2−} + UO_2^{2+} \rightarrow COT + UO_2 \qquad (2)$$

6509

dx.doi.org/10.1021/ic2026522 | *Inorg. Chem.* 2012, 51, 6507−6516
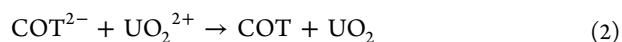
The thorium(IV) system cannot take part in such red-ox reactions. It would also be useful to study the formation of the uranium clusters from U(IV) sources only in the absence of the COT reduction system to pay for the reaction (such as in the synthesis of the cluster by controlled hydrolysis or pH change). The other possible thermodynamic factors of the clusters formation might be the tendency of actinyl dioxide molecules toward sintering, and the stabilization of the cationic clusters by anionic ligands, either bridging or not.

Thus, we consider the reactions shown in Table 1, using the neutral AnO_2 as an actinide-oxygen source and adding it to

Table 1. AnO_2 Dimerization^a Energies for Different Products' Spin States, As Computed with AE-L1 Method, kcal/mol

AnO_2	spin multiplicity	PBE	PBE0
$UO_2{}^b$	1 (pure)	−41.9	−8.4
	1 (broken)	−59.4	−57.6
	3	−56.3	−52.3
	5	−57.4	−56.8
ThO_2	1 (pure)	−93.1	−97.2

$^a2AnO_2 \rightarrow An_2O_4$. ^{b}The most stable, triplet state of UO_2 is used as an energy reference

other mononuclear An(IV) species. Again, following the works of Berthet et al. on the synthesis of tetraoctatetraenyl- and iodide-covered clusters, we chose the corresponding actinocenes and actinide tetra-iodides and their combinations (eqs 5 to 7) as the cosource of actinide. This would yield ligated $[An_6O_8]$ clusters with cyclooctatetraenyl and iodide ligands, as shown in Figure 1c−e). We will also use dianionic oxo-ligands as capping atoms to compensate for the cluster's positive charge, leading to the cluster $An_6O_8(O)_4$, $=An_6O_{10}$, shown in Figure 1b.

The small molecules, such as actinyl oxides, halides, and actinocenes, have been thoroughly studied both computationally and experimentally. In fact, actinocenes were one of the first actinide molecules treated by relativistic quantum chemistry (actually even by DFT, in form of X_α) methods, by Rösch and Streitwieser,[57] and have been the subject of computation studies several times since then.[48,58] Our PBE/AE-L1 calculations predict $U(COT)_2$ to be of triplet ground state, in agreement with these earlier studies.

Uranium(IV) tetraiodide, in the form of a dioxane complex, was shown to be a versatile synthetic uranium source.[59] It seems that it has not yet been modeled theoretically. According to our computations, at the PBE/AE-L1 level, ThI_4 has the geometry of a tetrahedron, with Th−I bond lengths of 2.943 Å. The triplet UI_4 molecule is distorted due to Jan−Teller effects and has 2.876 and 2.889 Å bonds with two different I−U−I angles, one of 111° and three of 107°. The bond orders are larger than 1, 1.36 for the thorium and 1.43 for uranium tetraiodides, correspondingly, which is typical for actinide halides as a result of the ligands' π-back-donation.

The thorium dioxide is bent; our AE-L1 computations yield the O−Th−O angle of 120.3°. It is well-known that dioxouranium cations VI and V are stable and linear due to participation of the f orbitals of the uranium in bonding with oxygens.[60,61] The same is true for the neutral dioxouranium-(IV), which is, unlike thorium dioxide, also linear, according to our scalar relativistic GGA DFT and ab initio RI-MP2 computations.[40] The electronic structure of the uranium

dioxide molecule was a subject of controversy in both experimental (ref 28 and references therein) and theoretical[29−31] studies. In CASPT2 studies[29,30] as well as in the more balanced relativistic Fock-space coupled-cluster studies,[31] it is now thought that the ground state of UO_2 likely belongs to a triplet $5f^17s^1$ state (rather than to a triplet $5f^2$ which is of a considerably higher energy). Our PBE/AE-L1 unrestricted SCF leads to a seemingly correct state, HOMO being of predominantly U s character, with admixtures of other orbitals, and HOMO−1 being a pure φ-5f orbital. Even so, we do not aim here to reproduce the correct electronic structure of such a multireference, open-shell molecule as UO_2 but, rather, to get a variationally stable, ground-state solution within the affordable approximation chosen in this work: scalar-relativistic method, all-electron unrestricted Kohn−Sham approach, GGA DFT. The GGA DFT has its well-known limitations stemming from delocalization errors[62] and general deficiencies of single-determinant methods, such as the over-repulsive sterical interactions' lack of dispersion interactions,[63−66] systematic under-estimation of band gaps in oxide solids, and, especially important in the case of low-valent uranium compounds, not always correct shell structures for open-shell d[67,68] and f elements. For a balanced description of the chemistry of the systems, the addition of a (much preferable, variable) fraction of exact Hartree−Fock exchange to GGA DFT is recommended. Even more, to describe the atomic shell structure, one has to use a carefully chosen functional, which would not necessarily be the best one for thermodynamics. There are developments in the direction of a universal DF of the Beck−Russel type functional, but for now they are unavailable for the all-electron, relativistic method we want to use.[69] Another ad hoc method for the description of d and f atomic shells popular in the solid state physics community is DFT+U. The method has difficulties in that its results depend critically on the value of the Hubbard U parameter; moreover, it is known to lead to a multiple local minima for SCF solutions.[70] This is problematic for structure/thermochemistry applications of our interest here.

Right now, we cannot afford all-electron hybrid, or range-separated hybrid DFT computations for the whole range of An_1 to An_{12} clusters. One could use a pseudopotential approach to reduce size of the computational problem. However, it is known that the pseudopotential approximation can itself alter energetics[43,40] and spin-states of the open-shell metallo-complexes and clusters.[67,68,71] We will give the VLC-ECP method a try for geometries and thermodynamics; however, we mainly use the accurate all-electron (AE) scalar relativistic method. Thus, we chose together with the AE method a reasonably accurate yet affordable GGA functional, PBE.[54] We have shown earlier that for certain thermochemistry problems of actinides (homolytic dissotiations, disproportionation reactions) where the oxidation state of the actinide changes, the GGA functionals in general and PBE in particular have rather large errors,[40] and thus the use of hybrid functionals is recommended. On the other hand, ligand exchange in actinyl complexes without a change of oxidation state, hydration energies, and such is reasonably well described with PBE.[27,25] We will further test the performance of the PBE functional below by comparing the energies of the dimer formation against the more reliable hybrid PBE0[72] functional and by comparing the PBE-optimized geometries with experimental data available for the $[An_6O_8]$ clusters.

First, we will consider the simplest associates of actinyl dioxides, the dimeric $(AnO_2)_2=An_2O_4$ clusters of U(IV) and

Th(IV). The actinide dioxide dimers, Th_2O_4 and U_2O_4, possess an important characteristic structural feature of the larger $An_6O_8X_n$ clusters—the (single) rhombic face with alternating actinide and oxygen atoms (Figure 1a). A significant structural difference shows up between the U_2O_4 and Th_2O_4 dimers (Scheme 1). The former is planar and has two distinct U–O

Scheme 1. Geometric Features of Selected Clusters: (a) Thorium vs. Uranyl Dimers and (b) Symmetric Fragment of Triacontahedron $An_{12}O_{20}^{8+}$ vs. Two Inequivalent Oxygens ("cube" and "bridge") in the Distorted $An_{12}O_{20}^{8+}$
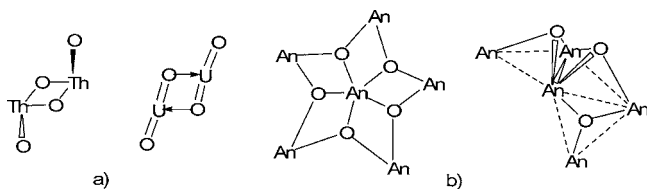
bonds (Tables 2 and 3). Thus, it can be seen as a dimer of two trans-uranyls(IV), retaining some of the uranyl character, not unlike the cation–cation interaction type dimers of uranyls(V) and (VI) studied by Pan et al.[73–75] On the other hand, the Th_2O_4 is an equilateral rhomb with the two capping oxo-groups pointing up and down the rhomb's plane. The out-of plane angle for these oxo-groups is 114.9° and 104.5° for the AE-L1 and VLC-ECP methods, correspondingly. The Th_2O_4 rhomb was studied very recently by Andrews et al., both experimentally and computationally, at the B3LYP level of theory with small-core ECPs[24] and was found to have a similar structure to that reported by our AE-L1 method.

For the uranium oxide dimer, there are several possibilities of the total spin. Each UO_2 monomer has two unpaired electrons. Thus, dimerization could lead to at least four states to consider: all-high-spin (quintet), triplet, true singlet, and a broken-spin (antiferromagnetic) singlet. We have considered all of these possibilities for our PBE/AE-L1 method. Moreover, for this model system, we have tried the corresponding hybrid DFT, PBE0/AE-L1 method, which could be more reliable. The UO_2 dimerization energies, leading to different spin states of U_2O_4 are shown in Table 1; we added the results for the thorium

analog, which is singlet, to compare PBE and PBE0 just for the case of dimerization energies. The absolute values of the dimerization energies for uranium and thorium dioxides are not too different between pure GGA and hybrid DFT, or at least GGA is not dramatically off, which justifies its use for the estimation of stabilities of the larger clusters.

For both of the density functionals, the all-high spin state, quintet of U_2O_4 is much more stable than the lower-spin triplet isomer and the pure, RHF singlet isomer. All of the uranyl dimers retain the same planar geometry, except that of the pure singlet, which has some butterfly type distortion (with the rhomb's O–U–U–O torsion angle of 156.1°). Unexpectedly, the broken spin, antiferromagnetic singlet with both uranium atoms having two unpaired electrons each is 2.06 kcal/mol more stable than the quintet at the PBE/AE-L1 level. This could be, at least in part, an artifact of GGA, which is known to have too delocalized f electrons, and thus perhaps spuriously predicting too much of U···U interaction. The inclusion of 25% of the exact exchange as in the PBE0/AE-L1 method makes the broken-spin singlet less stable, but still it is 0.8 kcal/mol more stable than the all-high-spin uranyl dimer.

A preference, however slight, for low-spin states of uranyl oxide clusters is unexpected—one would think that for the f elements, all-high spin, f states should be the most stable ones (c.f. however a recent work on magnetic coupling of the binuclear U(V) complexes[76]). To test the behavior for larger clusters, we computed corresponding broken-spin singlet isomers of selected larger uranium clusters (see Table S1). At least for the clusters that carry ligands, the all high-spin state is preferred, but note that for the UO_2 hexamer the broken-symmetry singlet is 5 kcal/mol more stable than the high-spin isomer. We must note that the magnetism of uranium oxide clusters is a complex question that requires further consideration. Our discussion is limited for the single-determinant, scalar-relativistic DFT method. Spin–orbit interaction and nondynamic correlation effects might well be needed for a more detailed and convincing study. Also, the possibility of "magnetic isomers" has to be considered for the less-than-high-spin clusters, which would greatly expand the number of the system under study, for the task is combinatorial. Thus, we will provide some data on one of the lower-spin systems, that is,

Table 2. Reactions of the actinide(IV) oxide cluster formation, and energies computed with PBE functional and different basis sets, kcal/mol

reaction, equation number	An = Th(IV)				An = U(IV)	
	AE-L1		VLC-ECP		AE-L1	
	ΔE	ΔG_{298}	ΔE	ΔG_{298}	ΔE	ΔG_{298}
$2AnO_2 \rightarrow An_2O_4$ (3)	−93.1	−79.2	−121.8	−107.4	−57.4	−55.5
$AnO_{2(linear)} \rightarrow AnO_{2(bent)}$ (4)	−7.8		−64.1		11.5	
$AnCOT_2 + 4AnO_2 + AnI_4 \rightarrow An_6O_8COT_2I_4$ (5)	−543.3	−466.9	−665.7	−588.0	−426.5	−374.5
$2AnCOT_2 + 4AnO_2 \rightarrow An_6O_8COT_4$ (6)	−495.2	−418.8	−600.8	−519.9	−379.0	−325.1
$2AnI_4 + 4AnO_2 \rightarrow An_6O_8I_8$ (7)	−538.8	−462.6	−653.7	−572.8		
$6AnO_2 \rightarrow An_6O_8(O)_4$ (8)	−511.2	−435.8	−617.8	−541.6	−388.9	−349.9
$An_6O_8(O)_4 + AnI_4 + AnCOT_2 \rightarrow An_6O_8COT_2I_4 + 2AnO_2$ (9)	−32.1	−31.1	−47.8	−46.4	−37.6	−24.5
$An_6O_8(O)_4 + An_6O_8COT_4 \rightarrow An_{12}O_{20}COT_4$ (10)	−11.3	1.7	−66.9	−52.5		
$An_6O_8^{8+} + An_6O_8(O)_4 \rightarrow An_{12}O_{20}^{8+}$ (11)	−760.0	−740.2	−820.1	−797.5		
$An_2O_4 + 2AnCOT_2 \rightarrow An_4O_4COT4$ (12)	−171.9	−147.9	−208.2	−180.1	−142.4	−114.0

Table 3. Selected Geometric and Electronic Parameters of the AnO$_2$ Monomer, Dimer, and High-Spin D$_{4d}$-Hexamer, Calculated at PBE/AE-L1 Optimized Geometries[a]

	ThO$_2$	Th$_2$O4	Th$_6$O$_{10}$	UO$_2$	U$_2$O$_4$[3]	U$_2$O$_4$[1c]	U$_6$O$_{10}$[13]	U$_6$O$_{10}$[1c]
$q(An)$[b]	0.93	0.88	0.77;0.92	0.7	0.73	7.5	0.77; 0.71	0.70;0.68
$q(O_{bridge})$[b]		−0.42	−0.37		−0.36	−0.43	−0.34	−0.33
$q(O_{actinyl})$[b]	−0.46	−0.46	−0.48	−0.35	−0.36	−0.32	−0.38	−0.38
spin on An[b]	0	0	0	2.04	2.17	±1.878	1.73; 2.71	±1.55; 1.62
HOMO α	−0.187	−0.195	−0.196	−0.138	−0.119	−0.128	−0.125	−0.135
LUMO α	−0.106	−0.099	−0.125	−0.133	−0.113	−0.112	−0.118	−0.123
LUMO β				−0.119	−0.106	−0.112	−0.136	−0.118
r (An=O)	1.907	1.907	1.907	1.815	1.836	1.831	1.852	1.848
b/o (An=O)	2.41	2.4	2.39	2.43	2.44	2.45	2.45	2.46
r(An−O)		2.177	2.440; 2.177		2.196; 2.019	2.165; 2.030	2.307; 2.203	2.14;2.33
b/o (An−O)		1.16	0.58;1.12		1.50; 0.87	1.45; 0.94	0.95; 0.69	1.05;0.64
ω (An=O)	807; 767	799; 798	802; 788; 788; 783	899; 814	832; 825	830; 824	820; 803; 802; 800	829; 813; 805; 805

[a]Distances are in Ångstroms; angles in degrees; charges, population bond orders, and HOMO and LUMO energies in atomic units. [b]Atomic charges and spin densities as computed with the Hirschfeld method [79] [c]Open-shell singlet with an equal number of U atoms with two unpaired α and two unpaired β electrons each.

Table 4. Geometric Parameters of Free Neutral An$_2$O$_4$ Dimers and Cationic An$_6$O$_8$$^{8+}$ and An$_{12}$O$_{20}$$^{8+}$ Clusters of Different Shapes, Calculated at PBE Optimized Geometries with Different Basis Sets[a]

cluster/	Th$_2$O$_4$		U$_2$O$_4$	Th$_6$O$_8$$^{8+}$		U$_6$O$_8$$^{8+}$
method	AE-L1	VLC-ECP	AE-L1	AE-L1	VLC-ECP	AE-L1
r(An−O)	2.177	2.238	2.196; 2.029	2.32	2.39	2.26
r(An···An)	3.446	3.481	3.342	3.84	3.95	3.73
r(O···O)	2.633	2.816	2.575	2.61	2.68	2.57
∠(O−An−O)	74.4	78.0	75.2	68.5	68.1	69.7
∠(An−O−An)	105.6	102.0	104.8	111.4	111.7	110.7

cluster/	Th$_{12}$O$_{20}$$^{8+}$−I		Th$_{12}$O$_{20}$$^{8+}$−II	Th$_{12}$O$_{20}$$^{8+}$−III[b]	U$_{12}$O$_{20}$$^{8+}$−I	U$_{12}$O$_{20}$$^{8+}$−II
method	AE-L1	VLC-ECP	AE-L1	VLC-ECP	AE-L1	AE-L1
r(An−O)	2.32	2.38	2.29 (cube); 2.25, 2.58 (bridge)	2.262; 2.298	2.26	2.25 (cube); 2.16, 2.62 (bridge)
r(An···An)	3.90	4.02	3.97; 3.62 (bridge)	3.827; 3.875	3.74	3.89 (cube); 3.45 (bridge)
r(O···O)	2.49	2.53	3.37 (cube); 2.60 (bridge)	2.327; 2.514	2.47	3.29 (cube); 2.52 (bridge)
∠(O−An−O)	64.9	64.3	94.8 (cube); 70.6 (bridge)		66.0	94.3 (cube); 71.1 (bridge)
∠(An−O−An)	114.9	115.5	119.8 (cube)		113.1	120.0

[a]Distances are in Ångstroms, angles in degrees. [b]Only the shortest contacts are shown.

broken-spin, antiferromagnetic singlets for U$_2$O$_4$ as well as the larger U$_6$O$_8$(O$_4$) hexamer (Table 3), for a comparison with the high-spin ones but will go no further in this direction. We will consider only all-high-spin energies for Table 2 and in the discussion below.

It would be instructive to compare the geometric parameters of the actinide oxide dimers, which are free from the additional angular strain that the rhombic faces of the hexanuclear clusters might have, with the ones of [A$_6$O$_8$] clusters. The geometries of all of the [A$_6$O$_8$] clusters optimized at the PBE/AE-L1 level retain the same rhombohedral character, despite changes in the ligands (see the Supporting Information for the geometries). The geometries are distorted from a completely symmetric rhombohedron by the ligands' influence. The largest distortion is observed for the polyoxide An$_6$O$_8$(O)$_4$, but even this cluster does not depart too far from the symmetric An$_6$O$_8$$^{8+}$ structure (Tables 3 and 4). Bond orders for the terminal oxo-groups of actinyl oxide dimers as well as hexamers retain the typical value of over 2 for both thorium(IV) and uranium(IV). The clusters' tricoordinated oxygen-to-actinide bonds have bond orders of about 1, indicating partially covalent character. The vibrational frequencies of the terminal oxo-groups of the dimer and hexamer clusters are within the usual range, characteristic of An=O frequencies. Interestingly, for the spin isomers of

uranium(IV) clusters, neither An=O or An−O bond orders nor An=O vibrational frequencies are much different between all-high-spin and broken-spin singlet isomers (Table 3).

The geometrical parameters for most symmetric, cationic An$_6$O$_8$$^{8+}$ clusters are provided in Table 4. In the case of thorium, we also compare the geometries by AE-L1 and VLC-ECP methods there. The rhomb in the oxide dimers has angles ∠(O−An−O) of around 75° and ∠(An−O−An) of about 105°, correspondingly. For the An$_6$O$_8$$^{8+}$ clusters, the former angle decreases down to 65−69°, and the latter increases up to about 111°. Bond lengths in the latter clusters are always larger than in the dimers, by 0.1−0.2 Å. Both angular and bond distance distortions do not seem to induce much of the strain, since we know that the [An$_6$O$_8$] clusters do exist.

As mentioned above, the ligands somewhat distort clusters, causing deviations from the regular rhombohedral cluster core and a lowering of symmetry. This complicates comparison with experimental X-ray data, because the data correspond to ligated and sometimes protonated clusters with a different ligand environment than ours. The partially protonated [Th$_6$O$_4$(OH)$_4$] cluster by Dixon et al. reportedly has Th−μ$_3$O bond lengths of 2.298(11) and Th−Th distances of 3.91−3.93 Å.[21]

For the uranium hexanuclear clusters, the partially protonated $[U_6O_4(OH)_4]$ geometry reported U–μ_3O of 2.211(10) to 2.271(11) Å, with U–U distances of 3.805(1) to 3.851(1).[17] The cluster prepared by Berthet et al. under nonaqueus conditions[14] has U–O of 2.205(13) to 2.332(2). The iodide-containing cluster has U–I distances of 3.087(16) to 3.175(16); the monocyclooctatetraenyl cluster has U–C distances of 2.724(16).

The values are in a reasonable agreement with our computed values, given the differences in actual ligand environment. The PBE/AE-L1 computed values are usually close for An–O but somewhat shorter for An–An distances. For the thorium systems computed with VLC-ECPs, we can see (Table 3) that this method systematically predicts all the bond lengths to be longer than those by the all-electron method. Comparing the bond lengths for thorium and uranium for both binuclear and hexanuclear clusters, we see that the uranium bonds are always shorter as a result of the actinide contraction. Uranium to iodide and cyclooctatetraenyl carbon distances, as given by PBE/AE-L1 calculations, are slightly shorter than the ones from the experiment: they are 2.67–2.69 Å for U–C(COT) and 2.98 Å for U–I in the $U_6O_8(COT)_2I_4$ cluster.

Going back to the energetics of the $[An_6O_8]$ clusters' formation from neutral AnO_2: in the gas phase, it is a highly exothermic process for all of the ligand combinations (Table 2, eqs 5–7). This is not so surprising since the gas-phase AnO_2 is a highly coordinative unsaturated species. Even the dimerization of these species releases a considerable amount of energy (see eq 3). For the thorium case, cluster formation energies are always more negative than for the uranium analogs. The process of exchange of the clusters' capping oxo-groups to COT and iodides as in eq 9 is mildly exothermic. The variations of the cluster formation energies, depending on the ligands and on the actinide metal, can be rationalized by a comparison of the corresponding thorium–ligand bond strengths. They reflect that uranium dioxide is more stable than the thorium one, and the situation is reversed for the corresponding tetra-iodides.

The difference of formation energies between thorium and uranium clusters that is shown in Table 2 can be, in large part, also attributed to the different nature of the source compound, actinide dioxide. The clusters are built of the rhombic units, which offer O–An–O angles (Table 4) that are closer to the bent thorium dioxide than the linear uranyl(IV) unit. In the latter case, the energy penalty that has to be paid for each UO_2 can be estimated by computing its bending energy to the same angle as for ThO_2 (Table 2, eq 4). Thus, forming the thorium clusters starting from ThO_2 is more exothermic than the uranium ones from UO_2. At the same time, the ligand exchange eq 9 is more favorable for the uranium, because there the more stable linear UO_2 unit is released. If we subtract the uranyl deformation energies for each uranyl involved, the cluster formation energies and ligand exchange energies for the uranium compounds get much closer to the thorium ones. For example, the energy of the dimerization of uranyl(IV) according to eq 3 would be −95.7 kcal/mol, and hexamerization (eq 8) would be −542.4 kcal/mol, correspondingly, which is still smaller but much closer to the reaction energies of the thorium analogs. The remaining energy differences between the uranium and thorium systems are due to the well-known actinide contraction, which leads to shorter but weaker An–O bonds along the actinide series.[77]

A comparison of the energies of dimerization and bending of dioxo-actinyls (Table 2, eqs 4 and 3 correspondingly) shows that VLC-ECP very strongly overestimates the stability of the dimers and the bent dioxothorium. (We note that the triple-ζ polarized basis for VLC-ECP is more flexible than the ANO–DZP quality basis we use for all-electron relativistic computations. So in the basis set limit, these two methods might get somewhat closer to each other.) Moreover, our attempt to compute UO_2 with the VLC-ECP method led to bent uranyl geometry similar to the ThO_2, which is clearly wrong. Given that the uranyl bending energy, as shown above, is an important factor in the oxide clusters stability, even for the thorium(IV) systems that do not have filled f shells, we would not recommend using the VLC-ECP methods for the production computations other than perhaps, some initial geometry optimizations. We note that the geometries optimized at the VLC-ECP level have systematic differences for thorium oxide clusters, overestimating all of the bond lengths (Table 3). We do not report further computations for our uranium systems with VLC-ECPs; for our test computations, they were giving the results for geometries and energies all too close to the thorium systems, missing the essential uranium chemistry.

Stability and Shape of the Clusters. As has been noted above, the most frequently obtained uranium(IV) oxide cluster, $U_6O_8^{8+}$, is a rhombohedron. That is, its faces are built from rhombi with alternating uranium and oxygen atoms. The latter possess a rather unusual tricoordinated mode, while uranium atoms are tetra-coordinated. The eight oxygen atoms form a cube in which the octahedron of six uranium atoms is embedded (Figure 1a)

At the same time, such an arrangement is the minimal fragment of the solid actinyl(IV) dioxides' so-called fluorite structure. The question is, which of these structural features would be important in the prediction of geometries of larger oxide clusters? Fused deca- and hexadeca-nuclear uranium oxide clusters that follow the space-filling fluorite structure were synthesized by Mazzanti et al. Yet it would be interesting to know whether highly symmetric, spherical clusters, akin to the uranyl peroxide family of Burns et al., could exist. We searched for the possible polyhedra built from rhombic faces with alternating U and O vertices. Such a family of polyhedra is known and is called zonohedra.[78] Rhombohedron is a case of zonohedron of the order $n = 4$, having 14 vertexes and 12 rhombic faces. The smaller member of the family of polyhedra is cube $n = 3$ (eight vertexes, eight square faces); the larger is $n = 6$, a rhombic triacontahedron with 32 vertexes (Figure 2). Given the requirement of having properly alternating actinide and oxygen atoms, for the polyhedra in Figure 2, it leads to stoichiometries of An_4O_4, An_6O_8, and $An_{12}O_{20}$, correspondingly. These clusters offer different oxygen-to-actinide ratios;

N=3, cube   N=4, rhombohedron   N=6, rhombic triacontahedron
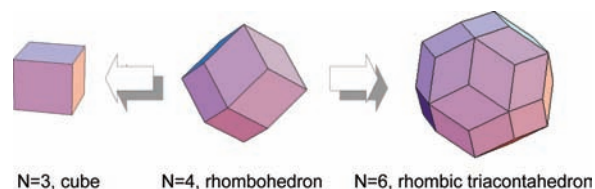
Figure 2. Higher ($N = 6$) and lower ($N = 3$) order zonohedra, rhombic triacontahedron and cube, correspondingly, that are similar to the rhombohedron ($N = 4$), which is shown in the middle.

but in all the cases, total charge dictated by the clusters' topology happens to be +8.

The DFT geometry optimizations were attempted for the naked $An_4O_4^{8+}$ and $An_{12}O_{20}^{8+}$ clusters starting from the idealized zonohedral guess structures. We were unable to locate a minimum corresponding to the free cubical $An_4O_4^{8+}$ clusters for either uranium or thorium. The likely reason is the high charge that destabilizes it, and the angular strain due to square faces having different angles from the rhombic ones. The $Th_{12}O_{20}^{8+}$ cluster did converge to a stationary point corresponding to the spherical, symmetric triacontahedron (Figure 3a). We name this type of structure $An_{12}O_{20}^{8+}$-I . But
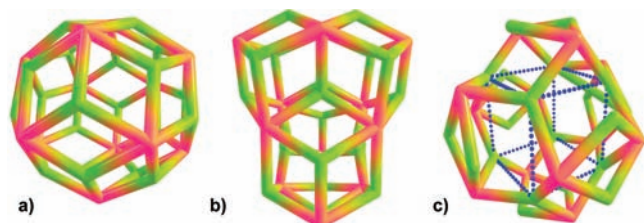
Figure 3. Isomeric $Th_{12}O_{20}$ clusters. (a) The right rhombic triacontahedron $An_{12}O_{20}^{8+}$-I, (b) the core similar to the one from refs 15 and 17 $An_{12}O_{20}^{8+}$-III, (c) distortion of the $Th_{12}O_{20}$ triacontahedron $An_{12}O_{20}^{8+}$-II. Thorium atoms are in pink, oxygen in green-yellow color; the blue dots mark inside cube in c.

the subsequent frequency computation showed that it is a saddle point. Reoptimization for minimum leads to another isomer, $An_{12}O_{20}^{8+}$-II, sitting 11.3 kcal/mol lower in energy (Figure 2b), which has been distorted from the zonohedral structure to form another symmetric polyhedron. In the latter, a cube of eight three-coordinating oxygens exists, just like in the hexanuclear cluster. The oxygens each join three neigbouring actinide atoms. All 12 actinide atoms form an icosahedron embedding the O8 cube. The icosahedron of Th12 is distorted because only eight of its faces contain the O8 oxygens. The rest of the oxygens exist in sort of dicoordinating bridging positions that sit on top of an An–An edge (Scheme 1).

The geometric parameters of regular triacontahedrae (which was also located for the uranium case with the AE-L1 method) $An_{12}O_{20}^{8+}$-I (Table 4, bottom rows) are not so different from those of the $[An_6O_8]$ clusters (Table 4, top rows). Yet the preferred structures are $An_{12}O_{20}^{8+}$-II, in which there are inequivalent actinides and oxygens with corresponding bond lengths both larger and smaller than in the zonohedral clusters. From these geometric parameters, there is no obvious reason why one arrangement must be preferred over another. It could be that the charge of the octa-cation dictates the need for eight such tricoordinated, partially more positively/less negatively charged oxygen atoms, to be equivalent while the rest of them are not, as in $An_{12}O_{20}^{8+}$-II, rather than delocalizing the charge over all the oxygens uniformly as in $An_{12}O_{20}^{8+}$-I. In the real situations of the condensed phase, there are ligands to balance the total charge, or hydrogens to protonate the remaining other oxygens, and thus the preference for the structure $An_{12}O_{20}^{8+}$-II that localizes eight positive charges to eight oxygens might change.

In order to check whether the compensation of charge might change the preferences for geometries of the clusters, we have attempted to compute optimized geometries of the ligated clusters for all of our zonohedrae, namely, $Th_4O_4(COT)_4$, $Th_6O_8(COT)_4$, and $Th_{12}O_{20}(COT)_4$. For all of them,

optimization converged to stationary structures (Figure 4). The tetranuclear cluster, which cannot be stable as the free
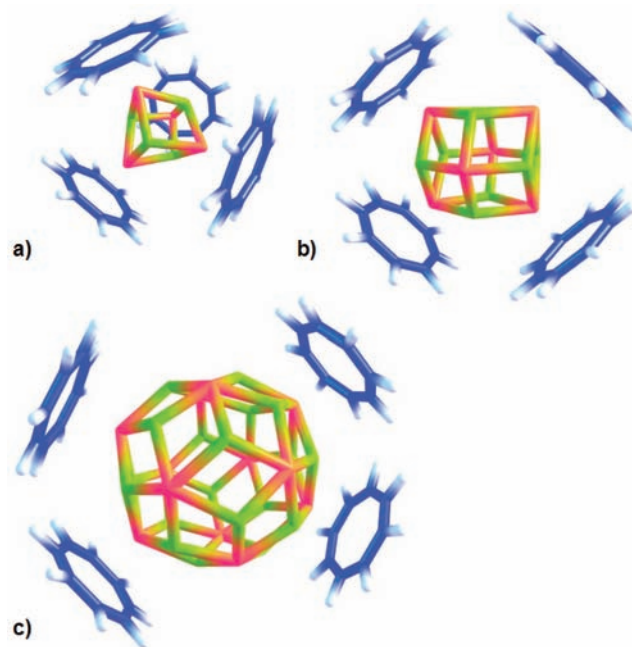
Figure 4. Neutral, tetra-cyctotoctatetraenyl clusters of various nuclearities, optimized at the PBE/AE-L1 level: (a) $Th_4O_4(COT)_4$, (b) $Th_6O_8(COT)_4$, (c) $Th_{12}O_{20}(COT)_4$. Oxygen atoms are in green-yellow, thoriums in pink, carbon in blue, hydrogen in light-blue color.

octa-cation, is a minimum in the ligated neutral form. It is notably distorted from the cube geometry, with two tetrahedra of Th4 and O4, the latter being smaller, and the faces not planar rhombi, unlike the ones in the larger clusters, especially the hexanuclear one. The energy of formation of the $Th_4O_4(COT)_4$, according to reaction 12, is very negative (Table 2), which again reflects the coordinatively unsaturated nature of either ThO_2 or its dimer. The similar uranium(IV) cluster can also be located as a minimum on the potential energy surface. Because of the preference for linear uranyl arrangements, as discussed above, its formation from the uranyl oxide dimer and uranocene is also highly exothermic, but less so than for the thorium analog.

The $Th_{12}O_{20}(COT)_4$ cluster has small imaginary frequencies related to rotation of the COT ligands around their axis, which we neglect here, but does not have any frequencies related to the change of the $[Th_{12}O_{20}]$ cluster core. As one can see, the ligated cluster (Figure 4c) has a somewhat distorted geometry of the triacontahedron, rather than the $An_{12}O_{20}^{8+}$-II type. Thus, the more symmetrical structures, perhaps, can be expected to exist in ligated forms, which would be not affected by the need to distribute the eight positive charges over 12 actinide, or 20 oxygen vertices—which seems to favor the less symmetric structure $An_{12}O_{20}^{8+}$-II over $An_{12}O_{20}^{8+}$-I.

It is interesting to note that the cluster obtained by Mazzanti et al. has a stoichiometry of $U_{12}O_{20}$ as well (we name it $An_{12}O_{20}^{8+}$-III). The experimentally obtained structure has multiple bridged ligands covering it and also is octa-protonated to match the excess negative charge. One can see that the double-decker prism-type cluster (shown in Figure 3c) is also built of rhombic, or at least tetragonal, faces with alternating uranium and oxygen vertices. In this way, it is similar to the

regular spherical triacontahedron (Figures 2c and 3a). However, in the Mazzanti cluster, uranium atoms are inequivalent—four of them are tetra- and four hexacoordinated. According to our VLC-ECP results, however problematic they are, for $Th_{12}O_{20}{}^{8+}$, the $An_{12}O_{20}{}^{8+}$-III cluster is 31.9 kcal/mol more stable than the distorted-spherical isomer $An_{12}O_{20}{}^{8+}$-II. The Th−O bond lengths in the $An_{12}O_{20}{}^{8+}$-III cluster (Table 4) can be similar or shorter than in the two other isomers.

But all in all, it seems that the structural motif of An−O−An−O rhombi is what determines the stoichiometry of this cluster, rather than its necessity to maintain fluorite-like space filling. The formation of the larger cationic cluster from the neutral and charged hexanuclear clusters via eq 11 (Table 2) is computed to be strongly exothermic for both thorium and uranium systems. Sintering of two ligated neutral thorium clusters into the larger dodecanuclear one via eq 10 is energetically favorable (however, the free energy of it is mildly exoergic, +1.7 kcal/mol for thorium). Thus, the formation of the larger clusters seems to be thermodynamically not unfeasible.

CONCLUSIONS

A relativistic DFT study was performed to study the thermodynamics of the existent clusters and to explore possible new actinide(IV)-oxide clusters of thorium and uranium. The building of the experimentally known $[An_6O_8]$ rhombohedral cluster is driven by the strongly exothermic sintering of the actinide dioxide particles. The clusters are stable as they are, in the absence of the bridging ligands. The anionic ligands, however, are needed to prevent the clusters from sintering or future growth. Our computations show that it is possible, because binding of the ligands such as the COT and iodide anions to the cluster is relatively stronger than that of the oxo-groups.

A key role in the stability of the oxide clusters is played by the nature of actinide. For thorium, where dioxide is bent, sintering into larger clusters is more likely than for the uranium where there is a penalty to be paid for necessary bending of the dioxouranium(IV) group. For the uranium systems, open-shell electronic configurations are always preferred; however, depending on the ligand environment (or its absence), the high spin, ferromagnetic isomers of the cluster might or might not be more stable than antiferromagnetic, broken-symmetry singlet isomers.

On the basis of the structural motif of the rhombic faces with alternating actinide and oxygen atoms, we have explored the possibility of the formation of other clusters besides $An_6O_8{}^{8+}$, trying regular polyhedra that would allow for similar faces (the zonohedra). The smallest case of a zonohedron—the free cationic tetranuclear cluster—was found to be unstable. However, for both uranium and thorium(IV), $[An_4O_4]$ clusters of distorted cubical shape can be stabilized by charge-compensating anionic ligands such as cyclooctatetraenyls. There are reasonably stable free cationic zonohedral (triacontahedronic) dodecanuclear clusters, in addition to experimentally studied hexanuclear ones and other spherical symmetric $[An_{12}O_{20}]$ structures.

We have found that a tricoordinated oxygen motif is characteristic for both hexa- and dodecanuclear octa-cationic clusters. Observing the importance of the rhombic faces formed by alternating actinide and the tricoordinated oxygens allows for the prediction of the new $[An_{12}O_{20}]$ structures as well as

offers an understanding of the stoichiometry of the double-prism $An_{12}O_{20}$ clusters studied experimentally.

We believe our relativistic DFT results support the computational evidence that there can be larger polyhedral clusters of actinyl(IV) oxides built of the same rhombic structural motifs, and that they might be promising synthetic targets for the preparation of new actinide(IV) nanoclusters.

■ ASSOCIATED CONTENT

Ⓢ Supporting Information
Tables with energy differences for high-spin and broken-spin singlet isomers of selected uranium oxide clusters. Optimized geometries of the free and ligated actinide oxide clusters studied in this work. This material is available free of charge via the Internet at http://pubs.acs.org.

■ AUTHOR INFORMATION

Corresponding Author
*E-mail: gas5x@yahoo.com.
Notes
The authors declare no competing financial interest.

■ ACKNOWLEDGMENTS

■ REFERENCES

(1) Burns, P. C.; Ikeda, Y.; Czerwinski, K. *MRS Bull.* **2010**, *35* (11), 868.
(2) Wang, S.; Alekseev, E. V.; Juan, D.; Casey, W. H.; Phillips, B. L.; Depmeier, W.; Albrecht-Schmitt, T. E. *Angew. Chem., Int. Ed.* **2010**, *49* (6), 1057.
(3) Alsobrook, A. N.; Hauser, B. G.; Hupp, J. T.; Alekseev, E. V.; Depmeier, W.; Albrecht-Schmitt, T. E. *Chem. Commun.* **2010**, *46* (48), 9167.
(4) Krivovichev, S. V.; Burns, P. C.; Tananaev, I. G.; Myasoedov, B. F. *J. Alloys Compd.* **2007**, *444*, 457.
(5) Unruh, D. K.; Burtner, A.; Pressprich, L.; Sigmon, G. E.; Burns, P. C. *Dalton Trans.* **2010**, *39* (25), 5807.
(6) Sigmon, G. E.; Ling, J.; Unruh, D. K.; Moore-Shay, L.; Ward, M.; Weaver, B.; Burns, P. C. *J. Am. Chem. Soc.* **2009**, *131* (46), 16648.
(7) Vlaisavljevich, B.; Gagliardi, L.; Burns, P. C. *J. Am. Chem. Soc.* **2010**, *132* (41), 14503.
(8) Miró, P.; Pierrefixe, S.; Gicquel, M.; Gil, A.; Bo, C. *J. Am. Chem. Soc.* **2010**, *132* (50), 17787.
(9) Rinehart, J. D.; Harris, T. D.; Kozimor, S. A.; Bartlett, B. M.; Long, J. R. *Inorg. Chem.* **2009**, *48* (8), 3382.
(10) Fox, A. R.; Bart, S. C.; Meyer, K.; Cummins, C. C. *Nature* **2008**, *455* (7211), 341.
(11) Rinehart, J. D.; Kozimor, S. A.; Long, J. R. *Angew. Chem., Int. Ed.* **2010**, *49* (14), 2560.
(12) Wyckoff, R. W. G. *Fluorite Structure Crystal Structures*; Interscience Publishers, New York, 1963; Vol. *1*, p 239.
(13) Berthet, J. C.; Thuery, P.; Ephritikhine, M. *Chem. Commun.* **2005**, *27*, 3415.
(14) Berthet, J. C.; Thuery, P.; Ephritikhine, M. *Inorg. Chem.* **2010**, *49* (17), 8173.
(15) Nocton, G.; Burdet, F.; Pecaut, J.; Mazzanti, M. *Angew. Chem., Int. Ed.* **2007**, *46* (40), 7574.

(16) Biswas, B.; Mougel, V.; Pecaut, J.; Mazzanti, M. *Angew. Chem., Int. Ed.* **2011**, *50* (25), 5744.

(17) Nocton, G.; Pecaut, J.; Filinchuk, Y.; Mazzanti, M. *Chem. Commun.* **2010**, *46* (16), 2757.

(18) Takao, S.; Takao, K.; Kraus, W.; Ernmerling, F.; Scheinost, A. C.; Bernhard, G.; Hennig, C. *Eur. J. Inorg. Chem.* **2009**, *32*, 4771.

(19) Soderholm, L.; Skanthakumar, S.; Wilson, R. E. *J. Phys. Chem. A* **2011**, *115* (19), 4959.

(20) Soderholm, L.; Almond, P. M.; Skanthakumar, S.; Wilson, R. E.; Burns, P. C. *Angew. Chem., Int. Ed.* **2008**, *47* (2), 298.

(21) Knope, K. E.; Wilson, R. E.; Vasiliu, M.; Dixon, D. A.; Soderholm, L. *Inorg. Chem.* **2011**, *50* (19), 9696.

(22) Braun, T. P.; Simon, A.; Ueno, F.; Bottcher, F. *Eur. J. Solid State Inorg. Chem.* **1996**, *33* (2–3), 251.

(23) Schimmelpfennig, B. From Molecules to Nanoparticles: A Computational Chemist's Point of View. In *Actinide Nanoparticle Research*; Kalmykov, S. N., Denecke, M. A., Eds.; Springer: Berlin, 2011; p 187.

(24) Andrews, L.; Gong, Y.; Liang, B.; Jackson, V. E.; Flamerich, R.; Li, S.; Dixon, D. A. *J. Phys. Chem. A* **2011**, *115* (50), 14407.

(25) Shamov, G. A.; Schreckenbach, G. *J. Phys. Chem. A* **2005**, *109* (48), 10961.

(26) Shamov, G. A.; Schreckenbach, G. *J. Phys. Chem. A* **2006**, *110* (43), 12072.

(27) Shamov, G. A.; Schreckenbach, G.; Martin, R. L.; Hay, P. J. *Inorg. Chem.* **2008**, *47* (5), 1465.

(28) Han, J. D.; Goncharov, V.; Kaledin, L. A.; Komissarov, A. V.; Heaven, M. C. *J. Chem. Phys.* **2004**, *120* (11), 5155.

(29) Gagliardi, L.; Heaven, M. C.; Krogh, J. W.; Roos, B. O. *J. Am. Chem. Soc.* **2005**, *127* (1), 86.

(30) Infante, I.; Andrews, L.; Wang, X. F.; Gagliardi, L. *Chem.—Eur. J.* **2010**, *16* (43), 12804.

(31) Infante, I.; Eliav, E.; Vilkas, M. J.; Ishikawa, Y.; Kaldor, U.; Visscher, L. *J. Chem. Phys.* **2007**, *127* (12), 124308.

(32) Shamov, G. A. *J. Am. Chem. Soc.* **2011**, *133* (12), 4316.

(33) Schreckenbach, G.; Shamov, G. A. *Acc. Chem. Res.* **2010**, *43* (1), 19.

(34) Shamov, G. A.; Schreckenbach, G. *J. Am. Chem. Soc.* **2008**, *103*, 13735.

(35) Dyall, K. G. *J. Chem. Phys.* **1994**, *100*, 2118.

(36) Laikov, D. N. *Chem. Phys. Lett.* **1997**, *281* (1–3), 151.

(37) Laikov, D. N. *Chem. Phys. Lett.* **2005**, *416* (1–3), 116.

(38) Laikov, D. N.; Ustynyuk, Y. A. *Russ. Chem. Bull.* **2005**, *54* (3), 820.

(39) Laikov, D. N. *An Implementation of the Scalar Relativistic Density Functional Theory for Molecular Calculations with Gaussian Basis Sets*, DFT2000 Conference, Menton, France, 2000.

(40) Shamov, G. A.; Schreckenbach, G.; Vo, T. N. *Chem.—Eur. J.* **2007**, *13* (17), 4932.

(41) Odoh, S. O.; Schreckenbach, G. *J. Phys. Chem. A* **2010**, *114* (4), 1957.

(42) Cao, X. Y.; Dolg, M. *Coord. Chem. Rev.* **2006**, *250* (7–8), 900.

(43) Batista, E. R.; Martin, R. L.; Hay, P. J. *J. Chem. Phys.* **2004**, *121* (22), 11104.

(44) Kuchle, W.; Dolg, M.; Stoll, H.; Preuss, H. *J. Chem. Phys.* **1994**, *100* (10), 7535.

(45) Moritz, A.; Cao, X.; Dolg, M. *Theor. Chem. Acc.* **2007**, *118* (5–6), 845.

(46) Moritz, A.; Cao, X. Y.; Dolg, M. *Theor. Chem. Acc.* **2007**, *117* (4), 473.

(47) Moritz, A.; Dolg, M. *Theor. Chem. Acc.* **2008**, *121* (5–6), 297.

(48) Moritz, A.; Doig, M. *Chem. Phys.* **2007**, *337* (1–3), 48.

(49) Laikov, D. N. *Priroda*; Moscow State University: Moscow, Russia, 2000.

(50) Energy-Consistent Pseudopotentials of the Stuttgart-Colgne group. http://www.theochem.uni-stuttgart.de/pseudopotentials/clickpse.en.html (accessed Aug. 1, 2011).

(51) Eichkorn, K.; Weigend, F.; Treutler, O.; Ahlrichs, R. *Theor. Chem. Acc.* **1997**, *97* (1–4), 119.

(52) Andrae, D.; Haussermann, U.; Dolg, M.; Stoll, H.; Preuss, H. *Theor. Chim. Acta* **1991**, *78* (4), 247.

(53) Turbomole Basis Set Library. In http://bases.turbo-forum.com/TBL/tbl.html (accessed May 2012).

(54) Perdew, J. P.; Burke, K.; Ernzerhof, M. *Phys. Rev. Lett.* **1996**, *77* (18), 3865.

(55) Ernzerhof, M.; Scuseria, G. E. *J. Chem. Phys.* **1999**, *110* (11), 5029.

(56) Adamo, C.; Barone, V. *J. Chem. Phys.* **1999**, *110* (13), 6158.

(57) Rosch, N.; Streitwieser, A. *J. Am. Chem. Soc.* **1983**, *105* (25), 7237.

(58) Li, J.; Bursten, B. E. *J. Am. Chem. Soc.* **1998**, *120* (44), 11456.

(59) Monreal, M. J.; Thomson, R. K.; Cantat, T.; Travia, N. E.; Scott, B. L.; Kiplinger, J. L. *Organometallics* **2011**, *30* (7), 2031.

(60) Dyall, K. G. *Mol. Phys.* **1999**, *96* (4), 511.

(61) Denning, R. G. *J. Phys. Chem. A* **2007**, *111* (20), 4125.

(62) Johnson, E. R.; Mori-Sanchez, P.; Cohen, A. J.; Yang, W. T. *J. Chem. Phys.* **2008**, *129* (20), 204112.

(63) Swart, M.; Sola, M.; Bickelhaupt, F. M. *J. Comput. Chem.* **2011**, *32* (6), 1117.

(64) Shamov, G. A.; Schreckenbach, G.; Budzelaar, P. H. M. *J. Chem. Theory Comput.* **2010**, *6* (11), 3442.

(65) Shamov, G. A.; Budzelaar, P. H. M.; Schreckenbach, G. *J. Chem. Theory Comput.* **2010**, *6* (2), 477.

(66) Schwabe, T.; Grimme, S. *Acc. Chem. Res.* **2008**, *41* (4), 569.

(67) Guell, M.; Luis, J. M.; Sola, M.; Swart, M. *J. Phys. Chem. A* **2008**, *112* (28), 6384.

(68) Swart, M. *J. Chem. Theory Comput.* **2008**, *4* (12), 2057.

(69) Becke, A. D.; Johnson, E. R. *J. Chem. Phys.* **2007**, *127*, 12.

(70) Meredig, B.; Thompson, A.; Hansen, H. A.; Wolverton, C.; van de Walle, A. *Phys. Rev. B* **2010**, *82* (19), 195128.

(71) Sakai, Y.; Miyoshi, E.; Klobukowski, M.; Huzinaga, S. *J. Chem. Phys.* **1997**, *106* (19), 8084.

(72) Adamo, C.; Barone, V. *J. Chem. Phys.* **2002**, *116* (14), 5933.

(73) Pan, Q. J.; Shamov, G. A.; Schreckenbach, G. *Chem.—Eur. J.* **2010**, *16* (7), 2282.

(74) Pan, Q.-J.; Schreckenbach, G.; Arnold, P. L.; Love, J. B. *Chem. Commun.* **2011**, *47* (20), 5720.

(75) Pan, Q.-J.; Schreckenbach, G. *Inorg. Chem.* **2010**, *49* (14), 6509.

(76) Meskaldji, S.; Belkhiri, A.; Belkhiri, L.; Boucekkine, A.; Ephritikhine, M. *C. R. Chim.* **2012**, *15* (2–3), 184.

(77) Andreev, G.; Budantseva, N.; Fedoseev, A.; Moisy, P. *Inorg. Chem.* **2011**, *50* (22), 11481.

(78) Taylor, J. E. *Am. Math. Mon.* **1992**, *99* (2), 108.

(79) Hirshfeld, F. L. *Theor. Chim. Acta* **1977**, *44* (2), 129.